

## Ice Age Winds: An Aquaplanet Model

GARETH P. WILLIAMS

*NOAA/Geophysical Fluid Dynamics Laboratory, Princeton University, Princeton, New Jersey*

KIRK BRYAN

*Program in Atmospheric and Oceanic Sciences, Princeton University, Princeton, New Jersey*

(Manuscript received 22 August 2005, in final form 16 December 2005)

### ABSTRACT

Factors controlling the position and strength of the surface winds during the Last Glacial Maximum (LGM) are examined using a global, multilevel, moist, atmospheric model. The idealized aquaplanet model is bounded below by a prescribed axisymmetric temperature distribution that corresponds to an ocean-covered surface. Various forms of this distribution are used to examine the influence of changes in the surface cooling and baroclinicity rates. The model omits seasonal variations.

Increasing the cooling lowers the tropopause and greatly reduces the moist convection in the Tropics, thereby causing a weakening and equatorward contraction of the Hadley cell. Such a cooling also weakens the surface westerlies and shifts the peak westerly stress equatorward. An extra surface baroclinicity in midlatitudes—implicitly associated with an increase in the polar sea ice—also shifts the peak westerly stress equatorward, but strengthens the surface westerlies.

Thus, calculations with combined surface cooling and baroclinicity increases, representative of the Last Glacial Maximum, reveal an absence of change in the *amplitude* of the peak westerly stress but exhibit a substantial equatorward shift in its *position*,  $7^\circ$  for a 3-K cooling and  $11^\circ$  for a 6-K cooling. The easterlies, however, always increase in strength when the surface westerlies move equatorward.

The application of these results to the LGM must take into account the model's assumption of symmetry between the two hemispheres. Any changes in the climate's hemispheric asymmetry could also cause comparable latitudinal shifts in the westerlies, probably of opposite sign in the two hemispheres. Published coupled-model simulations for the LGM give an equatorward shift for the peak westerlies in the Northern Hemisphere but give contradictory results for the Southern Hemisphere.

### 1. Introduction

This study examines how the atmosphere's circulation could have differed from its present form during the Last Glacial Maximum (LGM), as revealed by calculations with an idealized aquaplanet model subject to prescribed surface temperatures.

#### *a. The problem*

The detailed nature of climate change remains controversial, irrespective of whether the radiative heating increases or decreases. The scientific problem is com-

plex as it involves the circulation of both the atmosphere and the ocean, as well as processes in the cryosphere. Climate models have been developed that include most of the known important physical and dynamical elements in considerable detail. The recent simulations of the LGM climate using coupled ocean-atmosphere models (Hewitt et al. 2003; Kim et al. 2003) provide good examples of modern climate modeling.

Although such models include most of the well-known climate feedback mechanisms, they exclude a key process whose importance only became fully recognized during the last decade. The missing process involves the role played by carbon exchanges among the ocean, atmosphere, and terrestrial biosphere. The crucial importance of the carbon cycle in quaternary climate fluctuations is revealed by measurements of the carbon dioxide content of air bubbles trapped in the Antarctic ice cap (Petit et al. 1999).

---

*Corresponding author address:* Dr. G. P. Williams, NOAA/Geophysical Fluid Dynamics Laboratory, Princeton University, P.O. Box 308, Princeton, NJ 08542-0308.  
E-mail: Gareth.Williams@noaa.gov

There is no consensus, however, on the physical and chemical processes that might allow large changes to occur in the carbon reservoirs of the atmosphere, oceans, and biosphere. A decrease in the temperature of the ocean water provides an obvious mechanism as it would allow the ocean to take up larger amounts of carbon dioxide from the atmosphere. Although this effect is not considered sufficient to account for the very large changes observed, other mechanisms involving changes in the Southern Ocean circulation and in the sea ice distribution (Stephens and Keeling 2000) remain possible. Considering that both the ocean circulation and the sea ice distribution are very sensitive to the atmosphere's surface winds, any evaluation of the changes in the carbon dioxide uptake by the ocean during the LGM must involve the specifics of the ocean-atmosphere coupling. In particular, different surface wind and sea ice distributions are now considered to be important factors in the LGM carbon cycle.

#### *b. The procedure*

To address this last issue at a basic level, we now examine some of the processes that could be involved in determining the strength and location of the surface winds during the LGM. Although realistic coupled ocean-atmosphere models can do this with great generality, they are an overly complex tool for diagnosing the actual mechanisms involved in changing the atmospheric circulation. To remedy the situation, the present calculations are designed to be as simple as possible by using an idealized, global, multilevel, moist aquaplanet model, subject to prescribed surface temperatures. In particular, the lower boundary condition on the temperature assumes a zonal symmetry and neglects any seasonal variations, as well as explicit ice sheet effects. Such simplifications would not be justified for a fully coupled ocean-atmosphere model as the uptake and release of heat from the ocean's mixed layer is a highly nonlinear process. Nevertheless, our specified surface temperatures are based on values produced by such a fully coupled model.

Although simplifications are made, the atmospheric model retains the full effect of the water vapor, as well as a detailed specification of the cloud and radiation physics. As our solutions will show, changes in the atmospheric moisture content are of first-order importance in creating differences between the LGM and present climates, and thus cannot be neglected. We anticipate that the sensitivity of the climate to changes in the temperature depends strongly on the transition of the water from a gaseous to liquid and solid phases. We also assume that the lower boundary corresponds to an ocean at all latitudes. Since the ice provides an insulat-

ing layer, the surface air temperature lies well below the freezing point in polar regions. Thus the lower boundary condition corresponds to a prescribed surface air temperature (SAT) rather than to a sea surface temperature (SST).

To isolate the physical processes involved in changing the climate from the present to the LGM state, a variety of circulations are developed numerically by subjecting the aquaplanet model to a variety of SAT forms and CO<sub>2</sub> amounts. Changing the CO<sub>2</sub> amount, however, has little effect when the SAT is imposed rather than being computed by the model. An alternative approach would be to specify the ocean's poleward heat transport by using a static mixed layer model as a lower boundary condition, as in the study of Hewitt et al. (2003). However, there is no geological evidence to constrain estimates of the ocean's heat transport, and the various fully coupled models yield contradictory results.

The presentation begins in section 2 with a brief discussion of the numerical model. The interpretation of the solutions relating to the present and LGM states follows in section 3. The surface stress is emphasized as it is a crucial factor in the air-sea interaction that determines the climate regime. Then section 4 describes some intermediate states that lie between the present and LGM climates. The implications of the idealized model solutions are discussed and related to previous LGM modeling results while concluding in section 5. Although the model's assumption of interhemispheric symmetry at the surface limits any detailed application to the LGM,<sup>1</sup> the symmetry condition does make it easier to interpret the solutions.

## **2. Computational design**

The numerical calculations explore the sensitivity of the atmospheric circulation, particularly the surface winds, to certain changes in the cooling and the meridional temperature gradient of the lower boundary, as suggested by distributions from more complex studies using fully coupled ocean-atmosphere models.

#### *a. System of equations*

The numerical model is based on the Geophysical Fluid Dynamics Laboratory's (GFDL's) finite-difference atmospheric model (AM2) and is driven by a realistic radiative heating, moist convection, and SAT distribution (GFDL Global Atmospheric Model Development

---

<sup>1</sup> The degree of asymmetry may even have been greater during the LGM.

Team 2004).<sup>2</sup> Only the surface is simplified to that of a global ocean with preassigned temperatures. This so-called aquaplanet model predicts the zonal, meridional, and vertical velocity components ( $u$ ,  $v$ ,  $\omega$ ), plus the temperature and surface pressure fields ( $T$ ,  $p_*$ ), as a function of the latitude, longitude, and sigma vertical coordinates ( $\phi$ ,  $\lambda$ ,  $\sigma$ ), where  $\sigma = p/p_*$  is the normalized pressure. The model resolution has 24 vertical levels that favor the boundary layer and the tropopause, plus 90 latitudinal and 144 longitudinal evenly spaced grid points.

### b. Surface temperature functions

All flows are developed from an isothermal state of rest and are maintained by a radiative heating, with the insolation fixed at a distribution equivalent to a perpetual equinox, and by SATs with terms taken from the following function:

$$S(\phi) = [(25 \cos 2\phi + 10 \sin^2 2\phi) - (10 \sin^2 \phi + 6) + 273] \text{K}, \quad (1)$$

where the first pair of terms represents the present mean annual state, to give the *control* state (case A), and the second pair represents an extra midlatitude baroclinicity plus an additional global cooling that combine to give the *cold* LGM state (case B). These control and cold functions, shown in Fig. 1, are based on the simulated temperature distributions of Stouffer and Manabe (2003, their Fig. 3) for the Southern Hemisphere. The cases for the various forms of the SAT function and for the various  $\text{CO}_2$  amounts are listed in Table 1 and discussed in sections 3 and 4.

In presenting the solutions, the plotted fields are time-averaged quantities, based on zonal means sampled once a day. All calculations are extended for three years, with the contoured fields and the surface stresses being based on averages over the last four months and two years, respectively.

## 3. Climate calculations

### a. Climate of the control state

Analysis of the control circulation (case A) reveals the existence of a persistent wandering jet stream that resembles the Southern Hemisphere annular mode

<sup>2</sup> The AM2 model is adjusted to give an exact heat balance for the *observed* surface temperatures only. For our calculations, this leads to net global surface energy imbalances of 20–30  $\text{W m}^{-2}$ , a range that lies acceptably within the uncertainty level of the physics parameterization.

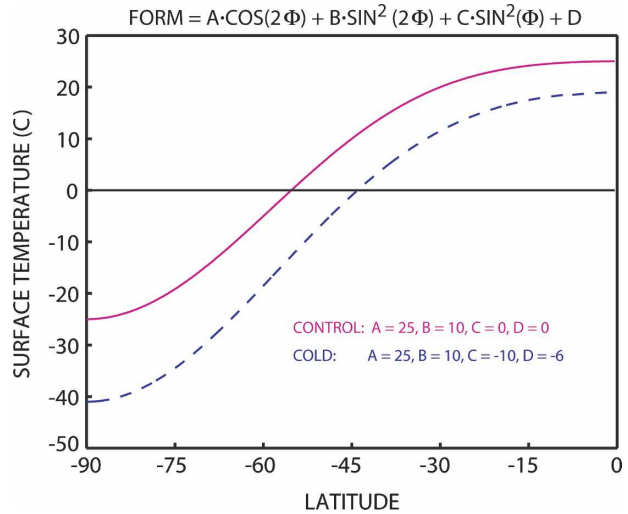


FIG. 1. Imposed latitudinal surface temperature distributions for the control and cold cases, A and B (solid and dashed curves).

(SAM) described by Thompson and Wallace (2000). The jet wanders on a longer time scale than do the synoptic-scale features, a behavior that Lorenz and Hartmann (2001) attribute to the stabilizing effect of the momentum convergence by the synoptic eddies. Although the variability of the jet is not a focus of this study—our focus is on the long-term mean position of the surface stresses—it exposes the sampling problem and indicates a need to average the fields over both hemispheres, using time integrations of the order of a year or more.

Furthermore, to improve the comparison between the data and the hemispherically symmetric solutions, we also combine the observed National Centers for Environmental Prediction (NCEP) fields for the two hemispheres. This involves a compromise, as the Northern Hemisphere, with its large land areas, is much warmer than the Southern Hemisphere. Thus it would be preferable to compare the model directly with the Southern Hemisphere. Such a comparison is limited, however, by the fact that the circulation of the Southern Hemisphere is greatly influenced by a thermal equator that lies in the Northern Hemisphere.

The mean NCEP and control temperatures are compared in Figs. 2a,c. The control temperature has a reasonably realistic latitudinal and vertical structure, though it is slightly colder than the NCEP global average and the tropopause is slightly lower. The control zonal flow is slightly stronger than the global NCEP flow at most heights (Figs. 2b,d) in keeping with the slightly stronger temperature gradients. Near the surface, the model and NCEP winds have their peak west-

TABLE 1. The magnitude and location of the maximum stress on the atmosphere at the surface, in pascals, for the eight cases driven by the various components of the SAT function [Eq. (1)], in degrees Kelvin, with differing amounts of CO<sub>2</sub>. Basic =  $25 \cos(2\phi) + 10 \sin^2(2\phi)$ ; extra baroclinicity (bc) =  $-10 \sin^2(\phi)$ ; extra cooling =  $(-15, -6, -3)$  K; control CO<sub>2</sub> = 356 ppm; low CO<sub>2</sub> = 165 ppm.

Case	Max stress	Latitude	State	Basic	Extra bc	Cooling	Low CO <sub>2</sub>
A	0.179	54°	Control	✓	—	—	—
B	0.162	44°	Cold	✓	✓	-6	✓
C	0.197	51°	Extra bc	✓	✓	—	—
D	0.118	50°	Cool	✓	—	-6	—
E	0.170	53°	Low CO <sub>2</sub>	✓	—	—	✓
F	0.179	43°	Cooler	✓	✓	-6	—
G	0.185	47°	Cooler	✓	✓	-3	✓
H	0.077	47°	Freezing	✓	—	-15	—

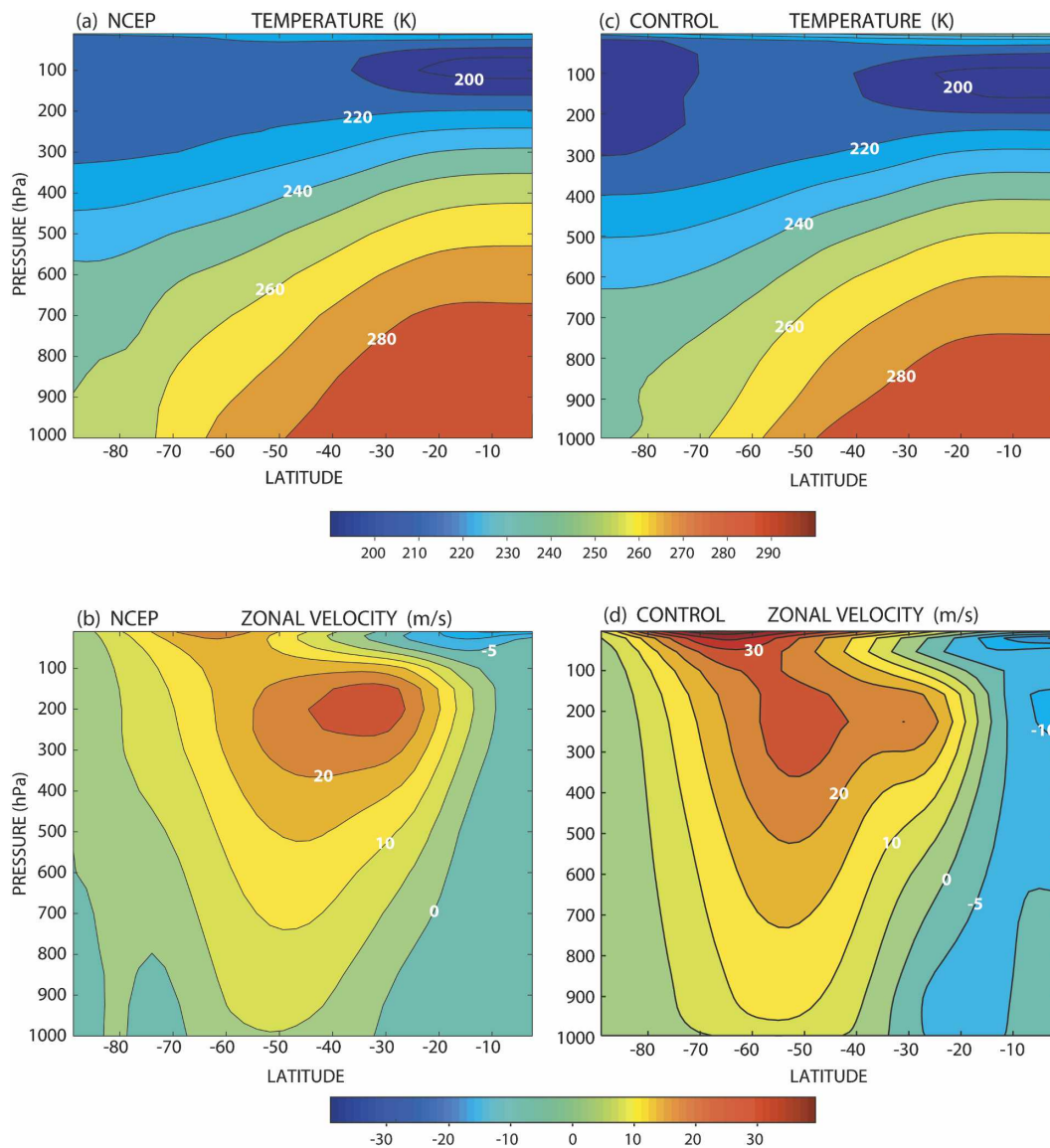


FIG. 2. Meridional distributions of the mean temperature and zonal velocity for the NCEP data and the control case A: (a) NCEP temperature, (b) NCEP zonal velocity, (c) control temperature, and (d) control zonal velocity. Contour intervals are (a), (c) 10 K, and (b), (d) 5 m s<sup>-1</sup>.

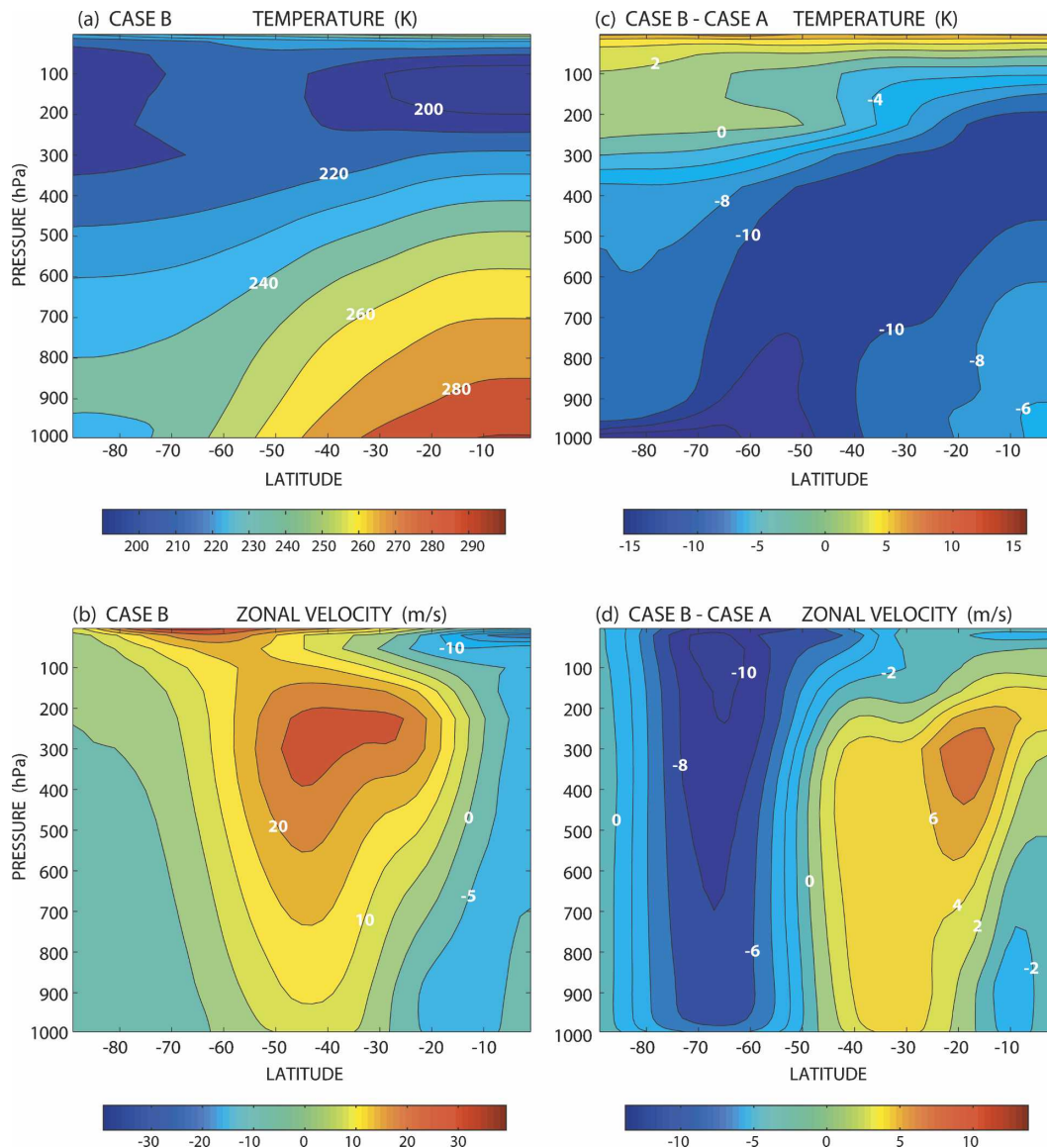


FIG. 3. Meridional distributions of the mean temperature and zonal velocity for the cold case B and their difference from the control case A values: (a) temperature, case B; (b) zonal velocity, case B; (c) temperature difference, case B minus case A; and (d) zonal velocity difference, case B minus case A. Contour intervals are (a) 10 K, (b) 5  $\text{m s}^{-1}$ , (c) 2 K, and (d) 2  $\text{m s}^{-1}$ .

erlies at approximately the same latitude, and the line separating the easterlies and westerlies is nearly the same. At the tropopause, the model's peak westerly is shifted slightly poleward. Given that the model assumes a fixed axisymmetric lower boundary condition, and a perpetual equinox, it is reassuring that the differences between the numerical and observed temperatures and zonal velocities are not greater.

#### b. Climate of the cold state

The cold state (case B) examines the effect of the additional (6 K) cooling and baroclinicity prescribed for

the SAT in (1). Note, however, that the presence of moisture and clouds in the model leads to more complex changes in the temperature field than the changes in the SAT profile alone imply. They result in a temperature structure (Fig. 3a) that displays a colder atmosphere with a much shallower troposphere, plus an inversion in higher latitudes. The difference between the temperatures of cases B and A shows that the region of warmer air in the Tropics and subtropics retreats to the deep Tropics, while the region of the arctic and subarctic regimes expands toward midlatitudes (Fig. 3c). The zone of peak temperature differences forms an arc that

approaches the surface in midlatitudes and moves equatorward with increasing height to reach the tropopause over the equator. In the stratosphere, the temperature difference between the two cases is reversed, with a general warming occurring as a result of the decrease in the  $\text{CO}_2$  amount. The stratospheric warming and the tropospheric cooling result in a general weakening of the tropical convection (and the related Hadley cell) and in a lowering of the tropopause.

The related zonal wind changes are dominated by a weakening of the westerlies in high latitudes and their strengthening in low latitudes (Figs. 3b,d).<sup>3</sup> In a colder climate, the vertical stability decreases as the lapse rate approaches the dry adiabat. At the same time, the latitudinal temperature gradient increases because of the contraction of the Hadley cell toward the equator. These two effects combine to give a much steeper meridional slope to the temperature surfaces in the Tropics. Other significant changes occur near the equator where a stronger baroclinicity causes the vertical wind shear to increase, resulting in the stronger easterlies at the surface and in the weaker easterlies aloft. This feature is important from the standpoint of the air–sea coupling and is discussed in section 3c. In the arctic zone, the polar easterlies prevail, even though they hardly exist in the control case.

Concerning its application to the LGM, the cold case with its enhanced cooling and baroclinicity could represent a state that occurs in the presence of an expanded sea ice cover. The global 6-K cooling in this case approaches the outer estimates for the LGM (Broccoli 2000) but remains useful, nonetheless, for isolating the processes involved. However, the latest geochemical data (Lea 2004) suggest that a cooling in the 3–4-K range may be more appropriate for the equatorial oceans during the LGM. Thus a related calculation, case G in Table 1, is made with the appropriate 3-K reduction and is discussed below in section 4. The model  $\text{CO}_2$  is also decreased for case B, but this has little impact as its effect is already included implicitly in the imposed cooler surface temperatures.

The change in the zonal velocity between the control and cold cases also has implications for climate change issues. For example, Thompson and Wallace (2000) suggest that the atmospheric circulation's response during a climate change can be described by the behavior of the first principal component of the SAM, as estimated for the zonal wind. Their mode has a rather

<sup>3</sup> The transient synoptic features vary little between the control and cold climates, a result supported by a parallel study of the dependence of the jet location on the tropopause height (Williams 2006).

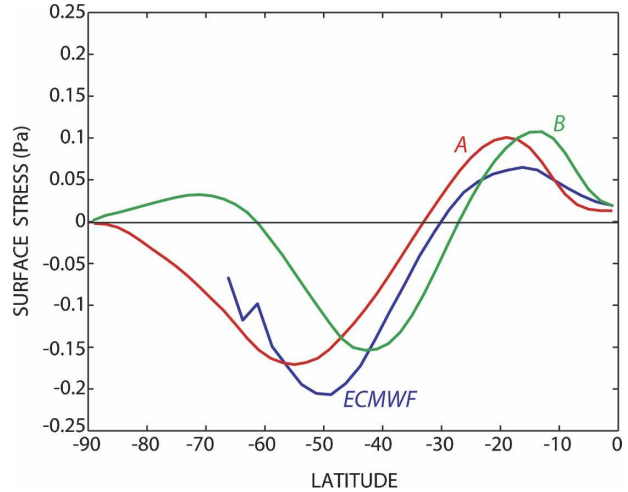


FIG. 4. Latitudinal profiles of the mean zonal wind stress on the atmosphere at the surface for the control (A) and cold (B) cases, compared against ECMWF forecasts for the Southern Hemisphere for the period 1980–86.

simple bipolar structure, with a nearly constant amplitude in height and with a nodal line that lies at 45° latitude. Here, however, the change between the two model cases has a more complicated, tripolar structure in which the midlatitude component is nearly constant with height and the two low-latitude components are stacked in the vertical (Fig. 3d). Of the latter pair, the upper component reflects the increase in the westerlies near the tropical tropopause, while the lower component reflects the strengthening of the trade winds. Overall, the change to a colder climate appears to produce a baroclinic response in the Tropics, thereby increasing the vertical wind shear, together with a barotropic response in midlatitudes.

### c. Surface stress

Comparing the zonal surface stress profiles for the two model cases against the Southern Hemisphere data, as compiled by Trenberth et al. (1990) from forecasts by the European Centre for Medium-Range Weather Forecasts (ECMWF), suggests (a) that the control values are realistic and (b) that they move 10° equatorward during the change to the cold state (Fig. 4). Figure 4 plots the stresses exerted on the atmosphere rather than on the ocean; hence the peak wind stress in the westerlies is negative and occurs near 50°S for the data. For the control case, the peak stress in the westerlies is weaker and occurs near 54°S—see also Table 1. For the cold case, the peak stress has the same magnitude as the control case but shifts equatorward to a 44°S location. In the easterlies, the stress and trade

winds are stronger for the cold case, particularly in the  $\phi = \pm 10^\circ$  equatorial region.<sup>4</sup>

The distribution of the westerly stress at the surface defines the sources and sinks of angular momentum. The global integral of these sources and sinks must vanish in a steady state, as integrating the curves of Fig. 4 confirms. The equatorward shift of the westerly wind stress in the cold case implies a greater torque, even without a change in the stress amplitude.<sup>5</sup> This means that the sink of angular momentum must be greater in the cold case. Thus, for global conservation, the source of the westerly angular momentum in the Tropics must increase. Since the torque becomes more uniform with respect to latitude near the equator, a balance can only be achieved by an increase in the easterly surface stress. Although the angular momentum constraint does not explain why the easterlies increase in amplitude for the cold case, it does confirm that stronger easterlies are consistent with the equatorward shift of the westerlies.

#### 4. Climates of intermediate states

The discussion in the previous section centers around the control and cold states of cases A and B, respectively. Now, we examine six variations (cases C–H) about these two states, to provide more insight into the model's dependence on the global cooling factor and the baroclinicity in the SAT formulation, as well as on the CO<sub>2</sub> amount. A concise view of the solutions is provided by Fig. 5, in which the amplitude and location of the peak westerly stress are plotted against each other, relative to the control case.

##### a. Single factor sensitivity

We begin with the four cases, C, D, E, and H, for which only one factor is changed from the control case (Table 1). For case C, only the imposed SAT gradient is altered, by strengthening it in midlatitudes. This produces a stronger (by 10%) wind stress and a modest (3°) equatorward shift in its location.

For case D, only the imposed SAT global-mean cooling factor is altered, being lowered by 6 K. This results in a 33% reduction in the stress amplitude and in a 4° equatorward shift in the peak stress. Both of these changes are influenced by the strong dependence of the moist processes on the absolute temperature, being as-

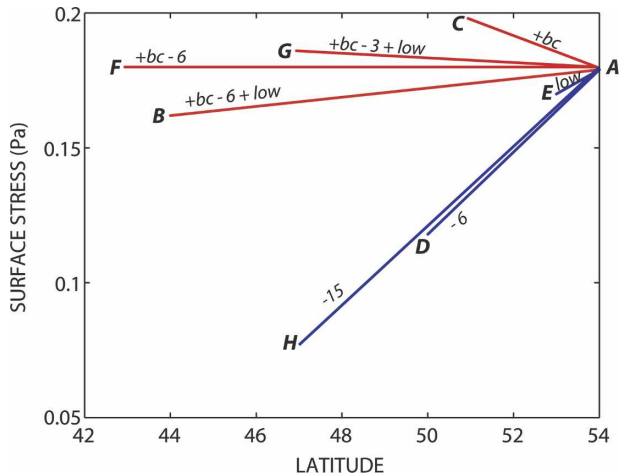


FIG. 5. Schematic summary for the control, cold, and intermediate (sensitivity) cases, showing changes in the amplitude and location of the maximum mean zonal wind stress on the atmosphere at the surface, relative to the control state. The case labels symbolize extra baroclinicity (+bc) and global cooling (–15, –6, –3) in the SAT, as well as low CO<sub>2</sub> levels.

sociated as they are with the weakening and equatorward retreat of the Hadley cell. For a dry atmosphere, the circulation would remain unaltered from case A.

Moist atmospheres behave quite differently from dry ones because of the sensitive dependence of the Clausius–Clapeyron relation on the value of the absolute temperature. A dry atmosphere would have nearly the same response to the same surface temperature gradients irrespective of the value of the mean temperature. Such a similarity does not exist for the present model as the moist processes are closely associated with the tropical convection and the strength of the Hadley cell.

This distinction between moist and dry atmospheres is supported by the nonintermediate case H, for which the global cooling is reduced by an unrealistic 15 K, primarily to eliminate the moist dynamical effect completely from the system. The weakened Hadley cell and jet result in a 56% reduction in the stress amplitude and in a 7° equatorward shift in the peak stress.

For case E, only the CO<sub>2</sub> content of the atmosphere is altered, to one-half the normal value. This leads to a slight decrease in the amplitude of the westerly wind stress and in a slight (1°) shift toward the equator. However, this is a somewhat unphysical case as the imposed SAT prevents the atmosphere from responding globally to the CO<sub>2</sub> change. Although the atmosphere can still respond to changes in the radiation pattern, the radiation must act alone without the usual large positive feedback from changes in the water vapor. As a result, the surface stress response is minimal, as are changes in the tropopause height and winds.

<sup>4</sup> Calculations with a fully coupled model by Bush and Philander (1998) also suggest that the easterlies were stronger during the LGM.

<sup>5</sup> This occurs because the distance to the rotational axis of the earth changes relatively rapidly over midlatitudes.

### b. Multiple factor sensitivity

Consider next the more complicated cases F and G, in Table 1, for which several parameters are changed, and for which the above simpler cases provide an interpretive guide.

Case F can be thought of as combining the elements of case C (with its enhanced baroclinicity) and case D (with its enhanced global cooling). Thus, if we simply combine the stress sensitivities of Fig. 5 for cases C and D in a linear way, we might expect a  $7^\circ$  equatorward shift and a 20% amplitude drop. However, case F exhibits no decrease in amplitude and a larger  $11^\circ$  equatorward shift. This indicates that the factors do not combine linearly. Comparing case F against case C implies that the major equatorward shift of the surface stress is primarily due to the extra 6-K cooling. Case F also exhibits the same major shrinking and equatorward retreat of the Hadley cell as case B.<sup>6</sup>

Case G documents a less extreme cold state than case F or B. For this, the global cooling is reduced by 3 K, rather than by 6 K, to match the recent estimate made by Lea (2004) from Ca–Mg isotope measurements in the equatorial Pacific. Despite the smaller cooling drop, the peak stress still shifts equatorward by a substantial  $7^\circ$  amount while gaining slightly in amplitude, relative to the control state.

Finally, from the four cases that have the same extra baroclinicity but different global cooling rates in the SAT, we conclude that both an extra baroclinicity and an extra global cooling are needed to produce a major latitudinal shift in the peak surface stress; acting singly, these factors produce a more modest shift.

### c. Physical interpretation

The solutions show that cooling the model atmosphere leads to a contraction of the easterlies and a shift in the westerlies, both toward the equator. It is physically reasonable that a cooling should decrease the lapse rate through a decrease in the atmospheric moisture—this effect has been noted in previous studies. Thus one would expect a lowering of the stratosphere due to the cooling, but not necessarily an equatorward shift in the zonal wind patterns.

To understand this behavior, we turn to the Hadley circulation theory of Held and Hou (1980). This theory assumes that the angular momentum is constant at the tropopause over the region of the Hadley cell, and that

<sup>6</sup> Note that case F is also equivalent to the cold case B without the reduced CO<sub>2</sub> amount and shows just how ineffective any CO<sub>2</sub> changes are in this model.

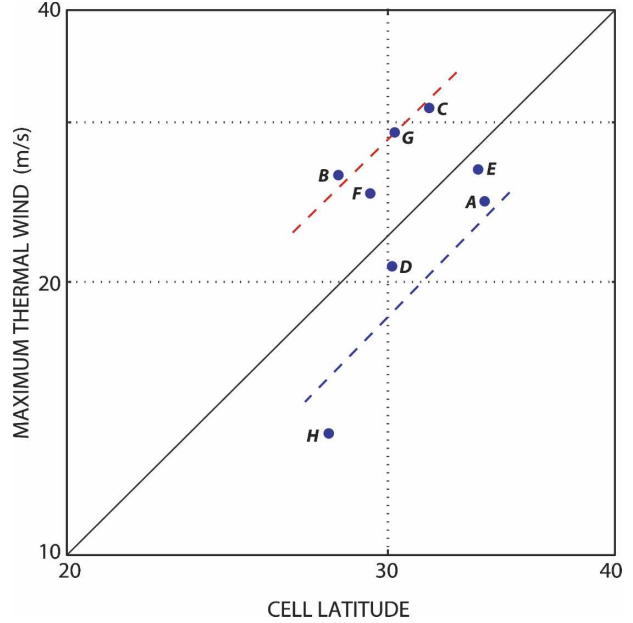


FIG. 6. The peak thermal wind as a function of the Hadley cell width, as measured by the latitude separating the easterlies and westerlies, for cases A–H in logarithmic coordinates. The results fall on two lines through the origin with slopes equal to 2. The lower line is for cases in which the surface baroclinicity matches that of the control case A. The upper line is for cases in which the surface baroclinicity matches that of the cold case B.

the temperature averaged over the entire Hadley cell is equal to the average temperature required by the radiative equilibrium. Combining these two constraints with geostrophy gives a simple relationship,

$$u_T \sim \phi_H^2, \quad (2)$$

between the thermal wind and the latitudinal width of the Hadley cell.

Plotting the maximum difference between the upper westerlies and the surface winds against the square of the latitude marking the boundary between the easterlies and westerlies reveals a considerable scatter in the relationship (Fig. 6). However, when the solutions are split into two groups the results are more consistent with (2). The cases clustered along the lower line have the same imposed SAT profile as the control form, while the cases along the upper line have the same extra baroclinicity. Both sets are consistent with the theory of Held and Hou (1980), although their sensitivity to the heating profile differs. The stronger the imposed surface baroclinicity, the more sensitive is the relationship between the thermal wind and the width of the Hadley cell. Variations in the width of the Hadley cell depend not only on changes in the absolute temperature but also on changes in the meridional SAT gradient and the

TABLE 2. The latitudinal wind shift over various oceans as defined by the difference between the LGM and control westerlies, from three recent simulations with coupled ocean–atmosphere models. The results of Shin et al. (2003) are based on the maximum surface wind stress, while the two others are based on the maximum surface winds.

Data	North Atlantic	North Pacific	Southern Ocean
Kitoh et al. (2001), their Fig. 4c	Equatorward	—	Poleward
Shin et al. (2003), their Fig. 6	Equatorward	Equatorward	Poleward
Kim et al. (2003), their Fig. 13	Equatorward	Equatorward	Equatorward

ensuing eddy fluxes. These results complicate the application of the theory to changing climates.

## 5. Conclusions

The calculations documented above are designed to examine the sensitivity of the atmospheric general circulation to a global cooling and a possible increase in the meridional temperature gradient, such as characterize the LGM in the simplest context. With this goal in mind, we have used a GFDL climate model that has a comprehensive water cycle and cloud and radiation physics, but also has the simplest possible boundary conditions. In particular, the surface air temperature (SAT) is chosen to be zonally symmetric and to have the same profile in each hemisphere. In addition, the insolation is fixed at a distribution equivalent to a perpetual equinox. By changing the form of the SAT in the aquaplanet model, it is possible to isolate the processes that cause shifts in the jet and surface drag between the present and the LGM states

The resulting solutions show that a cooling driven by a uniform lowering of the imposed surface temperature—without any changes in the SAT profile—causes a weakening of the westerly surface stress, as well as an equatorward shift of the surface westerlies. These changes are associated with a weakening and equatorward shrinking of the Hadley cell. But a strengthening of the westerly surface stress accompanies the equatorward shift of the surface westerlies when a change is made in the latitudinal SAT profile that imposes a stronger temperature gradient in midlatitudes—with or without an extra global cooling. Such a change could represent the influence of the enhanced sea ice extent of the LGM era.

The cooling acts to reduce the moisture to the extent that the weaker tropical convection results in a nearly dry adiabatic lapse rate rather than in a moist-adiabatic lapse rate. This effect lowers the tropopause and also reduces the thermal wind shear. The axisymmetric theory of Held and Hou (1980) predicts that a reduction of the thermal wind shear requires a corresponding reduction in the area occupied by the Hadley cell. The above solutions are consistent with this theory, al-

though certain details are sensitive to the exact form of the SAT latitudinal profile.

When both SAT factors are combined to examine the LGM climate, the tendencies to increase or decrease the surface westerlies tend to cancel, whereas the tendencies to shift the surface westerlies equatorward are approximately additive and thus result in a larger relocation. Together, they imply that for the LGM a cooling of 3 K at the equator and an increase in the temperature gradient (due to a more extensive sea ice cover) could give a significant 7° equatorward shift in the surface westerlies. In such a system (case G), the surface stresses in the easterlies are larger near the equator than in the control system (case A), even though the surface stresses in the westerlies have similar amplitudes. The results are consistent with the requirement that the angular momentum balance globally.

Our results also have some bearing on the interpretation of LGM simulations carried out with more complex, coupled ocean–atmosphere models. Table 2 summarizes the regional shifts in the surface westerly winds between the present and LGM states, as given by three recent studies with such models. For the Northern Hemisphere the coupled models agree with each other and with our idealized model, in that all display an equatorward shift.<sup>7</sup> For the Southern Hemisphere, however, the results are ambiguous, with two studies indicating a poleward shift in the surface westerlies, while the third study (Kim et al. 2003) displays an equatorward shift.

It is not obvious, however, that the LGM simulations listed in Table 2 have reached an equilibrium climate. Assuming that they have, the shifts obtained by Kim et al. (2003) are in the closest agreement with those of our idealized model. Not only are the displacements of the peak westerlies equatorward in both hemispheres, but the westerlies themselves are weaker than in the control climate. The easterlies, however, are stronger in the LGM simulations, again in agreement with the ideal-

<sup>7</sup> The aquaplanet model implies that such shifts are due, in equal amounts, to the global cooling and the stronger SAT gradient associated with an increased sea ice extent.

ized model. A more detailed quantitative comparison between results from the aquaplanet and various coupled models may be possible upon completion of the Paleo Modeling Intercomparison Project (PMIP-2).

Overall, our calculations imply that both an extra cooling and an extra baroclinicity in the SAT distribution produce significant equatorward shifts in the surface wind stress. Such winds could lead to significant changes in the ocean circulation and the climate during the LGM era. However, as a consequence of forcing both hemispheres symmetrically, any direct application of our results to the LGM climate must be limited. A shift in the position of the thermal equator during the LGM era could also have a strong effect on the position of the surface winds, as is suggested both by basic GCM studies (Hou and Molod 1995) and by more comprehensive models (Broccoli et al. 2006). Interhemispheric differences in the sea ice cover could have a similar effect (Langen and Alexeev 2004). The influence of such asymmetric forcing on atmosphere–ocean interaction is an important topic for future basic studies.

*Acknowledgments.* For contributions that made this study possible, we thank Isaac Held for advice, Bruce Wyman for model design, and Catherine Raphael for organizing the graphics. We are also indebted to Anthony Broccoli and the reviewers for perceptive comments that improved the presentation.

#### REFERENCES

- Broccoli, A. J., 2000: Tropical cooling at the Last Glacial Maximum: An atmosphere–mixed layer ocean model simulation. *J. Climate*, **13**, 951–976.
- , K. A. Dahl, and R. J. Stouffer, 2006: The response of the ITCZ to Northern Hemisphere cooling. *Geophys. Res. Lett.*, **33**, L01702, doi:10.1029/2005GL024546.
- Bush, A. B. G., and S. G. H. Philander, 1998: The role of ocean–atmosphere interactions in tropical cooling during the Last Glacial Maximum. *Science*, **279**, 1341–1344.
- GFDL Global Atmospheric Model Development Team, 2004: The new GFDL global atmosphere and land model AM2–LM2: Evaluation with prescribed SST simulations. *J. Climate*, **17**, 4641–4673.
- Held, I. M., and A. Y. Hou, 1980: Nonlinear axially symmetric circulations in a nearly inviscid atmosphere. *J. Atmos. Sci.*, **37**, 515–533.
- Hewitt, C. D., R. J. Stouffer, A. J. Broccoli, J. F. B. Mitchell, and P. J. Valdes, 2003: The effect of ocean dynamics in a coupled GCM simulation of the Last Glacial Maximum. *Climate Dyn.*, **20**, 203–218.
- Hou, A. Y., and A. Molod, 1995: Modulation of dynamic heating in the winter extratropics associated with the cross-equatorial Hadley circulation. *J. Atmos. Sci.*, **52**, 2609–2626.
- Kim, S.-J., G. M. Flato, and G. J. Boer, 2003: A coupled climate model simulation of the Last Glacial Maximum, Part 2: Approach to equilibrium. *Climate Dyn.*, **20**, 635–661.
- Kitoh, A., S. Murakami, and H. Koide, 2001: A simulation of the Last Glacial Maximum with a coupled atmosphere–ocean GCM. *Geophys. Res. Lett.*, **28**, 2221–2224.
- Langen, P. L., and V. A. Alexeev, 2004: Multiple equilibria and asymmetric climates in the CCM3 coupled to an oceanic mixed layer with thermodynamic sea ice. *Geophys. Res. Lett.*, **31**, L04201, doi:10.1029/2003GL019039.
- Lea, D. W., 2004: The 100 000-yr cycle in tropical SST, greenhouse forcing, and climate sensitivity. *J. Climate*, **17**, 2170–2179.
- Lorenz, D. J., and D. L. Hartmann, 2001: Eddy–zonal flow feedback in the Southern Hemisphere. *J. Atmos. Sci.*, **58**, 3312–3327.
- Petit, J. R., and Coauthors, 1999: Climate and atmospheric history of the past 420, 000 years from the Vostok ice core, Antarctica. *Nature*, **399**, 429–436.
- Shin, S.-I., Z. Liu, B. L. Otto-Bliesner, E. C. Brady, J. E. Kutzbach, and S. P. Harrison, 2003: A simulation of the Last Glacial Maximum using the NCAR–CCSM. *Climate Dyn.*, **20**, 127–151.
- Stephens, B. B., and R. F. Keeling, 2000: The influence of Antarctic sea ice on glacial–interglacial CO<sub>2</sub> variations. *Nature*, **404**, 171–174.
- Stouffer, R. J., and S. Manabe, 2003: Equilibrium response of thermohaline circulation to large changes in CO<sub>2</sub> concentration. *Climate Dyn.*, **20**, 759–773.
- Thompson, D. W. J., and J. M. Wallace, 2000: Annular modes in the extratropical circulation. Part II: Trends. *J. Climate*, **13**, 1018–1036.
- Trenberth, K. E., W. G. Large, and J. G. Olson, 1990: The mean annual cycle in global ocean wind stress. *J. Phys. Oceanogr.*, **20**, 1742–1760.
- Williams, G. P., 2006: Circulation sensitivity to tropopause height. *J. Atmos. Sci.*, in press.